MOL
PHARM

Photochemical Proteolysis of an Unstructured Linker of the GABA$_A$R Extracellular Domain Prevents GABA but Not Pentobarbital Activation

Ariele P. Hanek, Henry A. Lester, and Dennis A. Dougherty

Division of Chemistry and Chemical Engineering, Division of Biology, California Institute of Technology, Pasadena, California

Received July 27, 2009; accepted April 2, 2010

MOLECULAR PHARMACOLOGY

ABSTRACT

The GABA type A receptor (GABA$_A$R) is the major inhibitory receptor in the mammalian central nervous system and the target of numerous pharmaceuticals. The α-subunit of these pentameric Cys-loop neurotransmitter-gated ion channels contributes to the binding of both GABA and allosteric modulators such as the benzodiazepines, suggesting a role for this subunit in the conformational changes associated with activation of the receptor. Herein we use the nonsense suppression methodology to incorporate a photoactivatable unnatural amino acid and photochemically cleave the backbone of the α subunit of the $\alpha_1\beta_2$ GABA$_A$R in a linker region that is believed to span the subunit. Proteolytic cleavage impairs GABA but not pentobarbital activation, strongly suggesting that conformational changes involving this linker region are critical to the GABA activation pathway.

The GABA type A receptor (GABA$_A$R) is a member of the Cys-loop family of ligand-gated ion channels and mediates rapid inhibitory synaptic transmission in the mammalian nervous system. In addition to direct activation by the neurotransmitter GABA, the activity of GABA$_A$Rs can be allosterically modulated by a variety of compounds, including benzodiazepines (BZDs), barbiturates, volatile anesthetics, alcohols, and neuroactive steroids (Akabas, 2004). Identifying the mechanisms by which both GABA and these allosteric modulators affect the conformational movements within the GABA$_A$R is critical for understanding the underlying actions of these pharmaceuticals.

The GABA$_A$R shares a similar function and topology to the rest of the Cys-loop neurotransmitter-gated ion channel superfamily. At rest, GABA$_A$Rs are in a closed, nonconducting state. Binding of two molecules of GABA initiates a conformational change, termed activation, to an open, ion-conducting state. Each GABA$_A$R is composed of five homologous subunits arranged pseudosymmetrically around the central ion-conducting pore. In addition to numerous biochemical

studies, structural information relevant to these receptors has been provided by the crystal structure of the acetylcholine binding protein (Brejc et al., 2001) and the cryo-electron microscopy structure of the *Torpedo californica* nicotinic acetylcholine receptor (nAChR) (Unwin, 2005). Each subunit has a large extracellular amino terminal domain, followed by four membrane-spanning helices and a short extracellular carboxyl terminal tail. The extracellular domain consists of two antiparallel β sheets, with the β strands connected by unstructured loops that contribute to the ligand binding site (Corringer et al., 2000; Brejc et al., 2001) and to the activation pathway (Bouzat et al., 2004; Chakrapani et al., 2004; Xiu et al., 2005; Hanek et al., 2008).

GABA$_A$Rs are typically formed by assembly of α, β, and γ subunits, with the most prevalent form in the mammalian brain formed by α_1-β_2-α_1-β_2-γ_2 (Fig. 1). As seen with other Cys-loop receptors, maximal activation of the receptor requires the binding of two GABA molecules at interfacial binding sites defined by the β (primary binding elements) and α (complementary binding elements) subunits. Communication between these two binding sites is evidenced by Hill coefficients >1 seen in dose-response curves. The α subunit is unique in that it also contributes directly to the modulatory BZD binding site, located at the α/γ interface. Receptors lacking the γ subunit are also viable and, of course, unresponsive to BZDs. In the α-β-α-β-γ receptor, the binding of a BZD is believed to initiate an allosteric transition in the

ABBREVIATIONS: GABA$_A$R, GABA type A receptor; BZD, benzodiazepine; PB, pentobarbital; PCR, polymerase chain reaction; nAChR, nicotinic acetylcholine receptor; Npg, nitrophenylglycine; tRNA, transfer RNA; aa, amino acid.

protein that indirectly modifies the conformation of the GABA binding site (Changeux and Edelstein, 1998). This communication across the α subunit could also play a role in the intersubunit communication associated with the cooperativity of GABA binding.

Numerous mutagenesis and cysteine-labeling studies of α_1 have identified key residues in the complementary component of the GABA binding site and the BZD binding site. These residues can be associated with the canonical "loops" first identified in studies of the nAChR. His101 on loop A is essential to BZD binding (Buhr et al., 1996; Kucken et al., 2003; Berezhnoy et al., 2004), whereas a number of residues on loop E, beginning with Asn115, contribute to the complementary GABA binding component of the α subunit (Cromer et al., 2002; Kloda and Czajkowski, 2007). These residues are connected through a linker that is unstructured in both the acetylcholine binding protein and the cryo-electron microscopy nAChR structures. Binding at the GABA and/or the BZD site could influence the structure of this linker, propagating a structural change across the α subunit. This would allow direct communication between the GABA and BZD sites and could also contribute to intersubunit communication between the GABA binding sites.

In the present work, we disrupt this linker region and evaluate the impact on agonist-mediated receptor function in the $\alpha_1\beta_2$ GABA$_A$R. In particular, we use nonsense suppression (Nowak et al., 1995, 1998) to site-specifically incorporate the photoresponsive unnatural amino acid nitrophenylglycine (Npg) into this linker (England et al., 1997). Exposure to UV light then initiates photochemical cleavage of the GABA$_A$R backbone via a well precedented mechanism (Scheme 1). If communication across the α subunit is essential for receptor function, then cleavage of the linker back-

bone might be expected to alter the responsiveness of the receptor to agonist. Indeed, we find that photolysis leads to receptors that are unresponsive to GABA but are still activated by the noncompetitive agonist pentobarbital. The results suggest a critical role in receptor function for this unstructured, linker region.

Materials and Methods

Mutagenesis and Preparation of mRNA. Human α_1 and β_{2S} GABA$_A$R genes in pGEMHE were obtained from S.C.R. Lummis (Department of Biochemistry, University of Cambridge, Cambridge, UK). QuikChange polymerase chain reaction (Stratagene, La Jolla, CA) was used to make α_1Val107TAG, α_1Met111TAG, α_1Met113TAG, and α_1Pro114TAG mutants, and mutations were confirmed by sequencing. The cDNA was linearized using Nhe1 (Roche Diagnostics, Indianapolis, IN) for the α_1 subunit and either Spe1 or Sph1 (both from Roche) for the β_{2S} subunit. The mMessage mMachine kit (Ambion, Austin, TX) was used to generate capped mRNA for oocyte injection.

Oocyte Injection. Wild-type $\alpha_1\beta_{2S}$ mRNA was mixed in a 1:1 ratio and diluted to a final concentration of 100 ng/μl. Each oocyte was injected with 50 nl of mRNA mix, equivalent to 5 ng of mRNA mix. For suppression experiments, a 5:1 mix of the mRNA of the mutated α_1 gene and β_{2S} at a final concentration of 1 μg/μl was used. The mRNA mix was mixed in a 1:1 (v/v) ratio with the deprotected aa-tRNA. Each oocyte was injected with a total volume of 50 nl of RNA mix containing 25 ng of mRNA and 15 to 50 ng of aa-tRNA. After injection, oocytes were incubated for 24 to 48 h at 18°C before electrophysiology recordings. As controls, mRNA alone or mRNA mixed with dCA-tRNA (no unnatural amino acid attached) was injected into oocytes.

Characterization of Mutant Receptors. Peak GABA-induced currents were recorded at 22 to 25°C from individual oocytes using the OpusXpress system (Molecular Devices, Sunnyvale, CA). A stock solution of 10 mM GABA (Sigma-Aldrich, St. Louis, MO) in ND-96 buffer (96 mM NaCl, 2 mM KCl, 1 mM MgCl$_2$, 1.8 mM CaCl$_2$, and 5 mM HEPES, pH 7.5) was made fresh for each day's recording. Drug solutions were made from the stock by dilution in ND-96 buffer. Drug was delivered to cells via the automated pipette tips of the OpusXpress. Glass microelectrodes were backfilled with 3 M KCl and had resistances of 0.5 to 3.0 MΩ. The holding potential was -60 mV. To determine EC$_{50}$ values, GABA concentration-response data were fitted to the Hill equation (eq. 1), where I_{max} is the maximal peak current and n is the Hill coefficient:

$$\frac{I}{I_{max}} = \frac{1}{1 + (EC_{50}/[A])^n} \quad (1)$$

The biphasic dose-response relationship in Fig. 3 was fit using the modified Hill equation for biphasic data sets (eq. 2). I_{max} is the peak
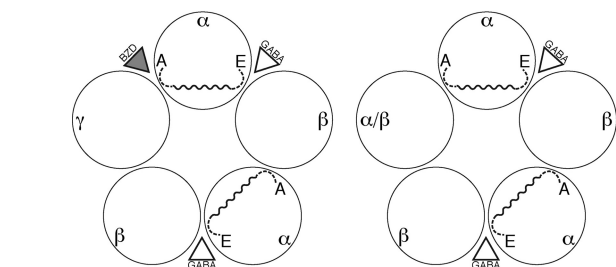
Fig. 1. Layout of the $\alpha\beta\gamma$ (left) and $\alpha\beta$ (right) GABA$_A$R. Loops A and E in the α subunits are indicated (broken lines) along with the unstructured linker (solid, wavy line) that is proposed to connect the two. The Npg mutation is incorporated into this linker. The α/β receptor is the subject of the present study.
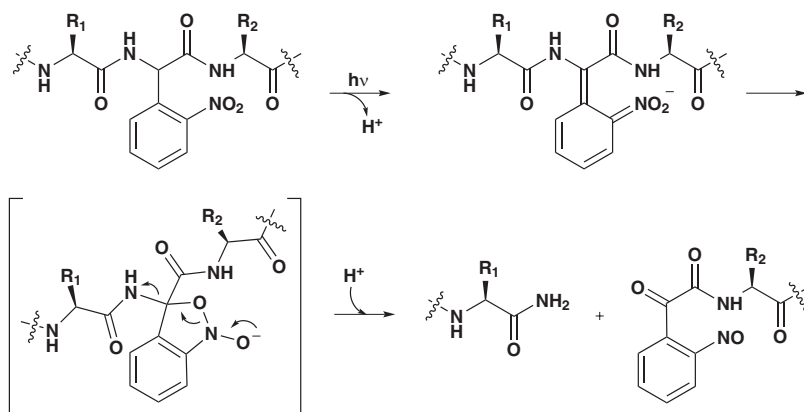
Scheme 1. Mechanism of Npg cleavage of the protein backbone.

current, c indicates the weighting coefficient for the lower portion, $EC_{50,1}$, $EC_{50,2}$, n_1, and n_2 refer to the lower and upper EC_{50} and Hill coefficients, respectively. The fit should be considered approximate and is subject to the choice of initial parameter values:

$$\frac{I}{I_{max}} = c\left(\frac{1}{1 + (EC_{50,1}/[A])^{n_1}}\right) + (1 - c)\left(\frac{1}{1 + (EC_{50,2}/[A])^{n_2}}\right) \quad (2)$$

The dose-response relationship for pentobarbital (purchased as pentobarbital chloride from Sigma-Aldrich) was determined in the same manner as for GABA. For concentrations of pentobarbital that caused channel block, the tail current was used to determine I_{max}. For the determination of I_{max} values from both GABA and pentobarbital (PB), a high dose of GABA was applied, followed by a saturating does of GABA (I_{GABA}) and then a saturating dose of PB (I_{PB}). PB solutions were stored at room temperature to minimize crystallization.

Oocyte Irradiation. Oocytes in ND-96 buffer containing theophylline, sodium pyruvate, and gentamicin (ND-96$^+$) and 4% horse serum were irradiated at 4°C in sterile 12-well polystyrene plates (Cellstar; Greiner Bio-One, Longwood, FL) with the lid in place. The irradiation source was a 288-W mercury lamp (BLAK-RAY Longwave Ultraviolet Lamp; Ultraviolet Products, San Gabriel, CA) equipped with a 360-nm band-pass filter at a distance of 15 to 30 cm for a total of 8 h unless otherwise indicated. The oocyte bath solution (ND-96$^+$ with 4% horse serum) was replaced every 1.5 to 2 h to avoid excessive heating. Nonirradiated oocytes were maintained at 18°C. Before electrophysiology measurements, irradiated oocytes were placed in fresh ND-96$^+$ with 4% horse serum at room temperature for at least 30 min. This led to more negative resting potentials and smaller leak currents but did not affect the dose-response relationships or I_{max} values.

Preparation of aa-tRNA. Met-tRNA was prepared as described previously (Nowak et al., 1995, 1998). In brief, methionine was protected using a nitroveratryloxycarbonyl group, and the carboxylic acid was activated as the cyanomethyl ester. The activated compound was coupled to the dinucleotide dCA, which was then enzymatically ligated to 74-mer THG73 tRNA$_{CUA}$ as detailed previously.

Npg-tRNA was prepared as described previously (England et al., 1997). Nitrophenylglycine was prepared according to published procedures (Davis et al., 1973; Muralidharan and Nerbonne, 1995; England et al., 1997). The amino group was protected with an I$_{2(aq)}$ labile 4-PO group (Madsen et al., 1995; England et al., 1997), the carboxylic acid was activated as the cyanomethyl ester, and the activated compound was coupled to the dinucleotide dCA, which was then enzymatically ligated to 74-mer THG73 tRNA$_{CUA}$ as detailed previously (Nowak et al., 1995, 1998).

The aa-tRNAs were stored with the amino groups protected. Before mixing the aa-tRNA with the mRNA mix, the aa-tRNA was deprotected. Methionyl-tRNA was deprotected by photolysis at 350 nm for 5 min. Npg was deprotected by mixing (1:1 by volume) Npg-tRNA with a saturated solution of aqueous iodine for 10 min at room temperature. One equivalent of mRNA mix was added to the deprotected aa-tRNA before injection. This yielded a total of 16.7 ng each of mRNA and Npg-tRNA per oocyte for Npg experiments and 25 ng each of mRNA and methionyl-tRNA per oocyte for wild-type recovery experiments.

Statistical significance of the mean I_{max} for oocytes exposed to UV light versus those that were not exposed to UV light was determined by the Student's t test of unpaired data with equal variance. A Student's t test of paired data with equal variance was used to compare the pentobarbital-induced and GABA-induced I_{max} values. A statistical comparison of I_{max} values between Npg-containing and non–Npg-containing receptors would not be meaningful because of likely differences in expression levels. Error values for EC_{50} values and Hill coefficients are standard errors of the mean, averaging values obtained from individual oocytes. A detailed discussion of the

reproducibility of these values in nonsense suppression experiments has been presented elsewhere (Torrice, 2009; Torrice et al., 2009).

Results

GABA Activation of αMet113Npgβ GABA$_A$R. The linker region of interest here (^{101}HNGKKSVAHNMTMPN) connects His101 to Asn115 in the α_1 subunit (Fig. 1). We evaluated four residues for Npg incorporation: Val107, Met111, Met113, and Pro114. The mutant Met113Npg (Fig. 2B) gave the largest expression levels in suppression experiments and functioned normally (Fig. 3, A and B) with only a modest decrease in EC_{50} (Table 1). In addition, this site performed well in two important control experiments. Injection into the *Xenopus laevis* oocyte of mRNA containing the TAG codon at α113 along with suppressor tRNA that did not have an amino acid appended gave only very small GABA-induced currents (<200 nA) compared with the ~2 μA currents seen when an amino acid is appended to the tRNA. This establishes that background reacylation of the tRNA cannot provide a major perturbation to our results. In addition, when methionine is appended to the suppressor tRNA (wild-type recovery), the receptors formed are identical to the conventionally expressed wild-type receptor in terms of shape of the dose-response relationship, the Hill coefficient, and the macroscopic currents. This establishes that the aminoacyl tRNA that is injected into the oocyte is not charged with another (natural) amino acid either by editing or by acylation of the tRNA after delivering its cargo. Were this to happen, the expressed receptors would contain a mixture of residues at the α113 site, rendering the methodology inapplicable. The αMet113Npgβ receptors did display lower I_{max} values than wild-type recovery, an issue discussed under *Discussion*.

Proteolytic Cleavage of αMet113Npgβ GABA$_A$. Oocytes expressing αMet113Npgβ GABA$_A$Rs were placed under a UV light source. Exposure time was monitored closely. Increasing the exposure time for oocytes expressing the αMet113Npgβ GABA$_A$R led to a substantial, progressive decrease in the macroscopic current (Table 2). After 8 h of exposure to UV light, the GABA-induced whole-cell currents for αMet113Npgβ had decreased such that the EC_{50} could not be accurately determined. These
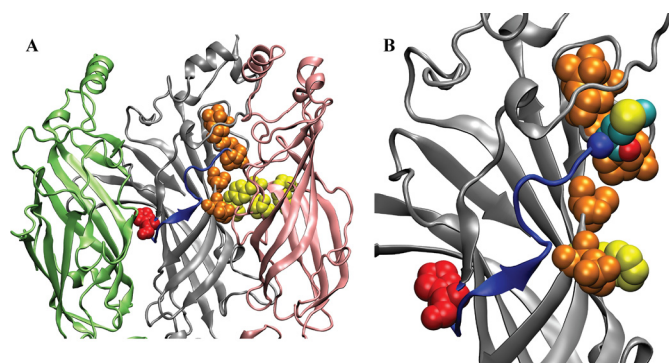
Fig. 2. An unstructured linker without defined secondary structure connects the GABA binding site and BZD binding site. A, the linker (blue) in the α subunit (gray) stretches from the β/α interface (β in pink) to the α/γ interface (γ in green). His101 (loop A residue) is shown in red. Yellow residues denote the aromatic box for GABA. Orange residues have been shown to be involved in GABA binding but are not part of the aromatic box. B, magnification of the linker region. Met113 is added (cyan) to mark the site where Npg is incorporated.

whole-cell currents had amplitudes similar to those of control experiments for oocytes injected only with mRNA and uncharged tRNA, suggesting that photolysis of Npg-containing receptors is complete after 8 h. Comparably long photolysis times have been required for complete photolysis in other studies using Npg (England et al., 1997). Oocytes expressing wild-type or αM113Mβ GABA$_A$Rs did not show similar variations in GABA-induced whole-cell current (Table 2) in response to exposure to UV light.

Repetition of these experiments, with evaluation only after 8-h exposure, verified the reproducibility of these

results (Table 3). On average, whole-cell current amplitude decreased by 89%. Despite the decrease in current size, the macroscopic currents of the αMet113Npgβ GABA$_A$R-expressing oocytes exposed to UV light (Fig. 3C) showed macroscopic waveforms that were qualitatively similar to those that were not exposed to UV light (Fig. 3A). Wild-type and αM113Mβ GABA$_A$Rs remained unchanged on exposure to UV light (Fig. 3, C and D; Table 3). Attempts to fit the small currents remaining after photolysis produced a biphasic dose-response curve (Fig. 3D), suggesting a heterogeneous population of remaining active receptors.

Fig. 3. Incorporation of methionine or Npg at αMet113 gives qualitatively similar macroscopic currents (A) and GABA dose-response relationships (B) to the wild-type receptor. Eight hours of exposure to UV light does not qualitatively alter the macroscopic kinetics (C) or GABA dose-response relationship (D) of wild-type GABA$_A$Rs. For oocytes expressing αMet113Npgβ GABA$_A$Rs, there is a statistically significant decrease in the magnitude of the macroscopic currents (C), although the overall shape of the trace remains the same. The dose-response relationship for receptors cleaved at αMet113 is biphasic (D). The biphasic fit was determined as described under *Materials and Methods*. Based on this fit, the two EC$_{50}$ values are 1 and 130 μM, respectively, for the bottom and top components of the curve. Where not visible, error bars are smaller than the marker.

TABLE 1

EC$_{50}$ values for wild-type recovery and Npg at αMet113

Errors are standard errors of the mean for averages of determinations for individual oocytes.

Receptor	EC$_{50}$	n_H	I_{max}	N
	μM		μA	
$\alpha\beta$ (wild type)	2.6 ± 0.3	1.25 ± 0.07	−4.2 ± 0.7	18
αMet113Metβ	2.7 ± 0.2	1.26 ± 0.03	−2.7 ± 0.4	32
αMet113Npgβ	0.57 ± 0.03	1.56 ± 0.04	−1.3 ± 0.1	25

TABLE 2

Increased exposure to UV light decreases the GABA-induced whole-cell current of oocytes expressing αM$\epsilon\tau$113Npgβ but not wild-type GABA$_A$Rs

Time	αMet113Npgβ		αMet113Metβ		$\alpha\beta$	
	I_{max}	N	I_{max}	N	I_{max}	N
	μA		μA		μA	
0 h	−2.3 ± 0.3	8	−2.1 ± 0.7	7	−9.8 ± 2.2	4
2 h	−0.6 ± 0.1	6	−2.6 ± 1.2	6	−6.6 ± 1.8	4
4 h	−0.32 ± 0.07	8	−1.22 ± 0.09	6	−8.9 ± 0.9	4
6 h	−0.20 ± 0.04	7	−1.3 ± 0.4	6	−8.4 ± 3.2	4
8 h	−0.11 ± 0.05	7	−2.3 ± 0.9	4	−3.9 ± 0.9	4

Pentobarbital Activation of the $\alpha\beta$ GABA$_A$R. The simplest explanation for the decrease in whole-cell current upon exposure of Npg-containing receptors to light is that backbone cleavage has rendered the receptors nonfunctional. However, other explanations are possible, including a photochemically induced decrease in the number of receptors on the surface of the oocyte or a decrease in the single-channel conductance of the receptor. To distinguish among these possibilities, we studied GABA$_A$R activation by the barbiturate pentobarbital. PB binds to a site different from GABA, probably in the transmembrane region of the β subunits (Amin and Weiss, 1993; Amin, 1999; Serafini et al., 2000). The single-channel conductance of PB-activated GABA$_A$Rs resembles that of GABA-activated receptors, suggesting that the open states of the ion channel have similar structures (Jackson et al., 1982; Rho et al., 1996). At low concentrations ($<100~\mu$M), PB modulates GABA-induced currents, whereas at higher concentrations, PB directly activates GABA$_A$Rs, and at still higher concentrations, it blocks the receptors. Studies using the substituted cysteine accessibility method with simultaneous fluorescence and electrophysiological recordings have established that PB activation of the GABA$_A$R elicits conformational changes in the GABA$_A$R that are distinct from those of GABA activation (Mercado and Czajkowski, 2008; Muroi et al., 2009).

If cleavage of the backbone by Npg leads to receptor endocytosis or a change in the single-channel conductance, one expects the maximal PB-induced currents to decrease with photolysis. However, if proteolysis at αMet113 simply prevents activation of the receptor by GABA, we anticipate that PB currents will remain the

same before and after photolysis. The PB dose-response relationships of wild-type and αMet113Npgβ GABA$_A$Rs were determined both before and after photolysis (Fig. 4). To reach saturation, concentrations of PB that block the receptor were necessary. In these cases, the peak of the tail current was used as the measurement (Fig. 4B).

The PB dose-response relationships for the αMet113Npgβ mutant before and after 8 h of irradiation were not qualitatively different from that of wild type (Fig. 4). The EC$_{50}$ values were similar for wild type, αM113Mβ, and αMet113Npgβ after photolysis (1400, 1700, and 1400 μM, respectively), as were the Hill coefficients (2.5, 2.3, and 2.4, respectively). The dose-response relationships indicate that in all three cases, 10 mM PB is sufficient to saturate the whole-cell current.

Agonist-induced macroscopic currents for wild-type GABA$_A$Rs were statistically similar in size for both agonists (Fig. 5 and Table 4) before and after UV exposure. These data indicate that PB is a full agonist for the wild-type receptor and, as expected, exposure of the wild-type channel to UV irradiation does not alter channel function. Proteolytic cleavage at αMet113 had no effect on PB-induced currents (Fig. 5 and Table 4), suggesting that the decrease in GABA-induced currents results not from endocytosis of the receptors or a change in the single-channel conductance but rather from a disruption to GABA binding and/or channel gating. It is noteworthy that the αMet113Npgβ mutant shows larger macroscopic currents for PB than for GABA, suggesting that the mutation lowers GABA but not PB efficacy.

Discussion

In the present work, we probe the consequences of cutting the protein backbone in a region of the α_1 subunit of the GABA$_A$R that appears as an unstructured, subunit-spanning linker in models of the receptor structure. As shown in Fig. 1, this linker is well positioned to provide direct communication between the GABA binding site and the proposed binding site of allosteric modulators such as benzodiazepines. In addition, this linker could provide communication across the α subunit to the interface with a β subunit, facilitating the coupling of the two binding sites that is a hallmark of these allosteric receptors.

To probe a possible functional role for this linker, we incorporated the unnatural amino acid Npg, enabling photo-

TABLE 3
Cumulative results of 8 h of UV exposure

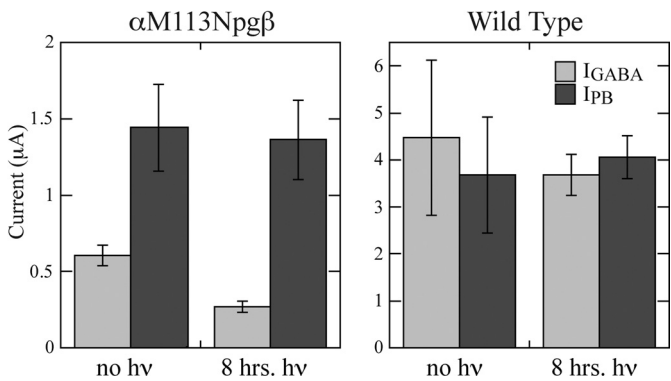|	Before UV		After 8-h UV	
	I_{max}	N	I_{max}	N
	μA		μA	
$\alpha\beta$	-9 ± 1	8	-5 ± 1	7
αMet113Met	-1.9 ± 0.5	9	-2.5 ± 0.7	5
αMet113Npg	-1.5 ± 0.2	23	$-0.17 \pm 0.03*$	24

* Statistically significant ($P < 0.01$) difference between the I_{max} value before and after 8 h of UV exposure. Similar comparisons between the wild-type ($\alpha\beta$) and αM113M data sets showed no significant differences. Higher expression of the wild-type receptor caused greater scatter in the I_{max} values. Although the I_{max} value after exposure to UV light is ~55% of the before UV light value, this range of expression levels for the wild-type receptor is normal for a given data set. Suppression experiments generally give less variability in expression size.
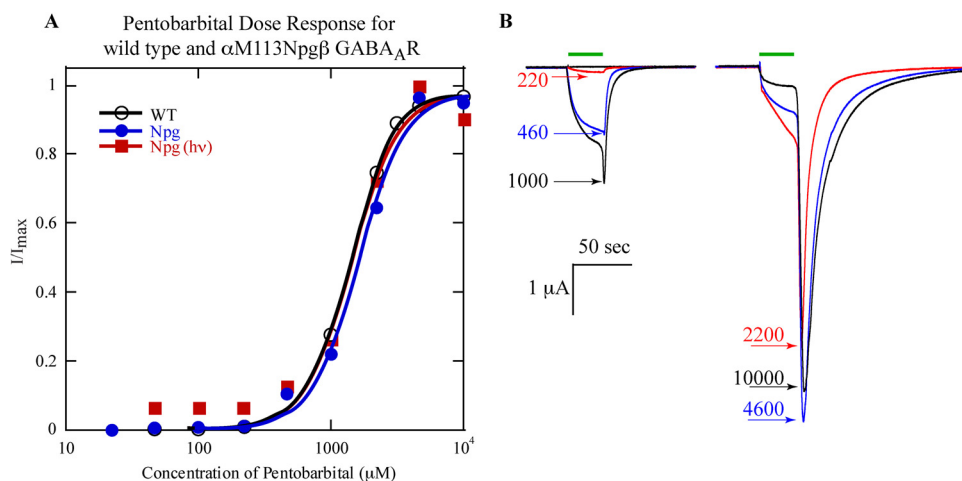
Fig. 4. A, pentobarbital dose-response relationships for wild-type and αMet113Npgβ (before and after photolysis) GABA$_A$R. B, PB-induced currents of wild-type GABA$_A$R. Concentrations are micromolar. Where not visible, error bars are smaller than the marker.

chemical cleavage of the backbone of the linker region. The αMet113Npgβ receptor functions normally before photolysis. Current levels seen for this receptor are smaller than what is seen when a conventional amino acid is incorporated by nonsense suppression. We might expect lower expression of the Npg mutant receptor because racemic Npg is appended to the tRNA, D-amino acids do not pass through the ribosome, and Npg is a β-branched amino acid, a structural type that sometimes incorporates less efficiently using the nonsense suppression methodology. At the same time, our studies of the noncompetitive agonist PB show that GABA-induced currents are less than PB-induced currents in the Npg mutant, whereas they are comparable in the wild-type receptor (Fig. 5). This suggests that GABA is a partial agonist in the mutant receptor, and this would also contribute to the lower current levels seen.

We find that photochemically induced proteolytic cleavage of the GABA$_A$R backbone at αMet113 is sufficient to prevent GABA activation of the receptor. This establishes a functional role in GABA activation for this linker. It is noteworthy that the fact that the cleaved receptor can still be activated with pentobarbital establishes that the backbone cleavage has not completely disrupted the structure of the receptor, and it has not induced substantial internalization of the receptor. One can imagine several ways in which cleavage of the linker would disrupt receptor function. Although αMet113 is fairly near the agonist binding site, no studies have defined this residue as being in a position to directly contact the agonist (Padgett et al., 2007), and it does not align with any of the residues that define the canonical "aromatic box" of the agonist binding site of Cys-loop receptors. In addition, the fact that the αMet113Npgβ receptor shows only a 5-fold shift in EC$_{50}$ (before photolysis) for what

must be considered a substantial side chain perturbation argues against this residue directly contacting GABA. Cleavage of the linker could indirectly affect GABA binding by inducing a conformational change that alters the shape of the binding site. Alternatively, the linker may be primarily involved in the gating pathway, coupling agonist binding to channel opening, consistent with other studies of this region of the receptor (Olsen, 1982; Kloda and Czajkowski, 2007) that implicate the linker region in the activation pathway of GABA$_A$R. At present, we cannot distinguish between these two possibilities: cleavage of the linker could alter the conformation of the agonist binding site, or it could disrupt the gating pathway. The essential result is clear: an intact linker is required for GABA-induced activation of the receptor.

We consider these data to be consistent with the available structural information indicating that, in the closed state, this region of the receptor lacks a defined secondary structure (Brejc et al., 2001; Unwin, 2005). If αMet113 was part of a well defined β-sheet or α-helix, the stabilizing backbone hydrogen bonding network might be expected to retain the overall structure after cleavage at a single backbone linkage, allowing the receptor to retain some function. We have seen just such behavior in the β-sheet region of the nAChR extracellular domain, in which a single disruption of backbone hydrogen bonding is well tolerated, but a double disruption leads to nonfunctional receptors (Gleitsman et al., 2009).

We noted above another possible role for this linker region, that of coupling the GABA site to the BZD site. However, given the results with the $\alpha_1\beta_2$ receptor, extending these studies to the $\alpha_1\beta_2\gamma_2$ GABA$_A$R is unlikely to provide additional information about GABA or BZD activation pathways. We have established a functional role for the linker region of the α subunit, and whereas introduction of the γ subunit might subtly alter activation by GABA (with no BZD present), it seems unlikely to suddenly make the α linker functionally irrelevant. As such, we fully expect that proteolytic cleavage of the α linker in the $\alpha_1\beta_2\gamma_2$ GABA$_A$R will be sufficient to prevent GABA activation of the receptor. BZDs modulate GABA-induced changes in the GABA$_A$R, and without GABA activation, experiments on photochemical proteolysis in this region would not be informative for BZD effects. Thus, a role for this linker in allosteric modulation by BZDs remains a tantalizing option that will have to be probed by other methods.

Fig. 5. Macroscopic whole-cell currents induced by saturating doses of GABA (light gray) or PB (dark gray). Left, PB-induced currents are unchanged by proteolytic cleavage of the αMet113Npgβ mutant. Right, control experiments with the wild-type receptor.

Acknowledgments

TABLE 4

In oocytes expressing αMet113Npgβ, PB-induced macroscopic currents remain constant despite 8 h of UV irradiation

	Before UV Exposure			After UV Exposure		
	I_{GABA}	I_{PB}	N	I_{GABA}	I_{PB}	N
	μA			μA		
αMet113Metβ	-4 ± 2	-4 ± 1	6	-3.7 ± 0.4	-4.1 ± 0.5	6
αMet113Npgβ	-0.61 ± 0.07	$-1.4 \pm 0.3^{\dagger}$	12	$-0.27 \pm 0.04^{*}$	$-1.4 \pm 0.3^{\dagger}$	12

* Statistical difference for values compared before and after UV exposure ($P < 0.01$), in which the reference state is before UV exposure.
† Statistical differences for GABA versus PB within a grouping ($P < 0.01$), in which GABA is used as the reference state.

References

Akabas MH (2004) GABAA receptor structure-function studies: a reexamination in light of new acetylcholine receptor structures. *Int Rev Neurobiol* **62:**1–43.

Amin J (1999) A single hydrophobic residue confers barbiturate sensitivity to gamma-aminobutyric acid type C receptor. *Mol Pharmacol* **55:**411–423.

Amin J and Weiss DS (1993) GABAA receptor needs two homologous domains of the beta-subunit for activation by GABA but not by pentobarbital. *Nature* **366:**565–569.

Berezhnoy D, Nyfeler Y, Gonthier A, Schwob H, Goeldner M, and Sigel E (2004) On the benzodiazepine binding pocket in GABAA receptors. *J Biol Chem* **279:**3160–3168.

Bouzat C, Gumilar F, Spitzmaul G, Wang HL, Rayes D, Hansen SB, Taylor P, and Sine SM (2004) Coupling of agonist binding to channel gating in an ACh-binding protein linked to an ion channel. *Nature* **430:**896–900.

Brejc K, van Dijk WJ, Klaassen RV, Schuurmans M, van Der Oost J, Smit AB, and Sixma TK (2001) Crystal structure of an ACh-binding protein reveals the ligand-binding domain of nicotinic receptors. *Nature* **411:**269–276.

Buhr A, Baur R, Malherbe P, and Sigel E (1996) Point mutations of the alpha 1 beta 2 gamma 2 gamma-aminobutyric acid(A) receptor affecting modulation of the channel by ligands of the benzodiazepine binding site. *Mol Pharmacol* **49:**1080–1084.

Chakrapani S, Bailey TD, and Auerbach A (2004) Gating dynamics of the acetylcholine receptor extracellular domain. *J Gen Physiol* **123:**341–356.

Changeux JP and Edelstein SJ (1998) Allosteric receptors after 30 years. *Neuron* **21:**959–980.

Corringer PJ, Le Novère N, and Changeux JP (2000) Nicotinic receptors at the amino acid level. *Annu Rev Pharmacol Toxicol* **40:**431–458.

Cromer BA, Morton CJ, and Parker MW (2002) Anxiety over GABA(A) receptor structure relieved by AChBP. *Trends Biochem Sci* **27:**280–287.

Davis AL, Smith DR, and McCord TJ (1973) Synthesis and microbiological properties of 3-amino-1-hydroxy-2-indolinone and related compounds. *J Med Chem* **16:**1043–1045.

England PM, Lester HA, Davidson N, and Dougherty DA (1997) Site-specific, photochemical proteolysis applied to ion channels in vivo. *Proc Natl Acad Sci USA* **94:**11025–11030.

Gleitsman KR, Lester HA, and Dougherty DA (2009) Probing the role of backbone hydrogen bonding in a critical beta sheet of the extracellular domain of a cys-loop receptor. *Chembiochem* **10:**1385–1391.

Hanek AP, Lester HA, and Dougherty DA (2008) A stereochemical test of a proposed structural feature of the nicotinic acetylcholine receptor. *J Am Chem Soc* **130:**13216–13218.

Jackson MB, Lecar H, Mathers DA, and Barker JL (1982) Single channel currents activated by gamma-aminobutyric acid, muscimol, and (−)-pentobarbital in cultured mouse spinal neurons. *J Neurosci* **2:**889–894.

Kloda JH and Czajkowski C (2007) Agonist-, antagonist-, and benzodiazepine-induced structural changes in the alpha1 Met113-Leu132 region of the GABAA receptor. *Mol Pharmacol* **71:**483–493.

Kucken AM, Teissére JA, Seffinga-Clark J, Wagner DA, and Czajkowski C (2003) Structural requirements for imidazobenzodiazepine binding to GABA(A) receptors. *Mol Pharmacol* **63:**289–296.

Madsen R, Roberts C, and Fraserreid B (1995) The pent-4-enoyl group—a novel amine-protecting group that is readily cleaved under mild conditions. *J Org Chem* **60:**7920–7926.

Mercado J and Czajkowski C (2008) Gamma-aminobutyric acid (GABA) and pentobarbital induce different conformational rearrangements in the GABA A receptor alpha1 and beta2 pre-M1 regions. *J Biol Chem* **283:**15250–15257.

Muralidharan S and Nerbonne JM (1995) Photolabile "caged" adrenergic receptor agonists and related model compounds. *J Photochem Photobiol B* **27:**123–137.

Muroi Y, Theusch CM, Czajkowski C, and Jackson MB (2009) Distinct structural changes in the GABAA receptor elicited by pentobarbital and GABA. *Biophys J* **96:**499–509.

Nowak MW, Gallivan JP, Silverman SK, Labarca CG, Dougherty DA, and Lester HA (1998) In vivo incorporation of unnatural amino acids into ion channels in *Xenopus* oocyte expression system. *Methods Enzymol* **293:**504–529.

Nowak MW, Kearney PC, Sampson JR, Saks ME, Labarca CG, Silverman SK, Zhong W, Thorson J, Abelson JN, and Davidson N (1995) Nicotinic receptor binding site probed with unnatural amino acid incorporation in intact cells. *Science* **268:**439–442.

Olsen RW (1982) Drug interactions at the GABA receptor-ionophore complex. *Annu Rev Pharmacol Toxicol* **22:**245–277.

Padgett CL, Hanek AP, Lester HA, Dougherty DA, and Lummis SC (2007) Unnatural amino acid mutagenesis of the GABA(A) receptor binding site residues reveals a novel cation-pi interaction between GABA and beta 2Tyr97. *J Neurosci* **27:**886–892.

Rho JM, Donevan SD, and Rogawski MA (1996) Direct activation of GABAA receptors by barbiturates in cultured rat hippocampal neurons. *J Physiol* **497:**509–522.

Serafini R, Bracamontes J, and Steinbach JH (2000) Structural domains of the human GABAA receptor 3 subunit involved in the actions of pentobarbital. *J Physiol* **524:**649–676.

Torrice MM (2009) *Chemical-Scale Studies of the Nicotinic and Muscarinic Acetylcholine Receptors*, California Institute of Technology, Pasadena, CA.

Torrice MM, Bower KS, Lester HA, and Dougherty DA (2009) Probing the role of the cation-pi interaction in the binding sites of GPCRs using unnatural amino acids. *Proc Natl Acad Sci USA* **106:**11919–11924.

Unwin N (2005) Refined structure of the nicotinic acetylcholine receptor at 4A resolution. *J Mol Biol* **346:**967–989.

Xiu X, Hanek AP, Wang J, Lester HA, and Dougherty DA (2005) A unified view of the role of electrostatic interactions in modulating the gating of Cys loop receptors. *J Biol Chem* **280:**41655–41666.

Address correspondence to: Dr. Dennis A. Dougherty, 1200 E California Blvd., M/C 164-30, Pasadena, CA 91125. E-mail: dadougherty@caltech.edu